Supporting Information

"Ionic Liquids based Variable Focus Lens"

Xiaodong Hu,[a] Shiguo Zhang,[b] Chao Qu,[a] Qinghua Zhang,[b] Liujin Lu,[b] Xiangyuan Ma,[b] Xiaoping Zhang*,[a] and Youquan Deng*,[b]

[a]*School of Information Science and Engineering, Lanzhou University, Lanzhou, China*
[b]*Centre for Green Chemistry and Catalysis, Lanzhou Institute of Chemical Physics, CAS, Lanzhou, China*
Email: ydeng@licp.cas.cn; zxp@lzu.edu.cn

1. Synthesis and Characterization of ILs.

Nine imidazolium ILs with different cation and anion structures (Figure S1), namely, 1-ethyl-3-methylimidazolium perchlorate ([EMIm][ClO_4]), 1-butyl-3-methylimidazolium perchlorate ([BMIm][ClO_4]), 1-butyl-3-methylimidazolium trifluoromethylsulfonate ([BmIm][CF_3SO_3]), 1-ethyl-3-methylimidazolium dicyanamide ([EmIm][$N(CN)_2$]), 1-ethyl-3-methylimidazolium bis(trifluoromethanesulfonyl)amide ([EmIm][NTf_2]), 1-butylpyridinium tetrafluoroborate ([BPy][BF_4]), 1-ethyl-3-methylimidazolium nitrate ([BmIm][NO_3]), 1-ethyl-3-methylimidazolium tetrafluoroborate ([EMIm][BF_4]), 1-ethyl-3-methylimidazolium hexafluorophosphate ([BMIm][PF_6]), were synthesized in our laboratory according to the established procedures.

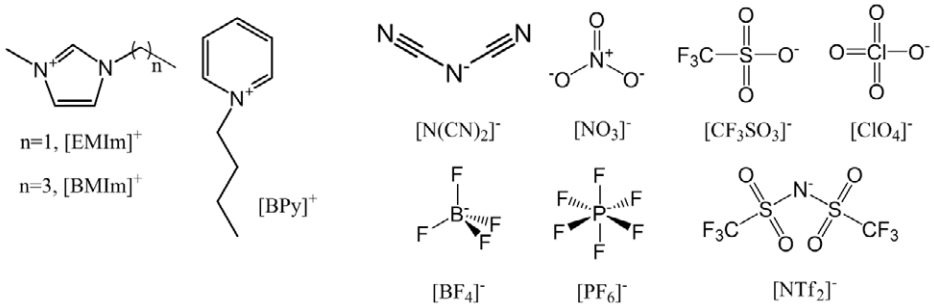

Figure S1. Formulas and structures of the ionic liquids studied.

Prior to measurements all ILs were dried in vacuo at 80 °C for 3 h, except [EMIm][$N(CN)_2$], which dried in vacuo at 60 °C for 3 h. The water content is ~160 ppm for [EMIm][ClO_4], ~182 ppm for [BMIm][ClO_4], ~200 ppm for [BPy][BF_4], ~22 ppm for [EMIm][NTf_2], ~190 ppm for [EMIm][$N(CN)_2$], ~104 ppm for [BMIm][CF_3SO_3], and ~200 ppm for [BMIm][NO_3], ~287 ppm for [EMIm][BF_4], ~122 ppm for [BMIm][PF_6].

The ion conductivity was measured using a Mettler-Toledo Seven Muliti meter. The refractive index was measured using DR-M2 abbe refractometer (ARTAGO (Japan)). The viscosity was measured on a Brookfield DV-III+ viscometer. The surface tension was measured on a surface/interface analytical device (Solon Tech. (shanghai)) using the Du Noüy ring method. Contact angle data was obtained by a SEO Contact Angle Measuring Device (PHOENIX 300). The water content was determined by Karl-Fisher analysis (Metrohm KF coulometer). The thicknesses of the insulating and hydrophobic layer were measured by a surface profiler (Micro-XAM, USA). The UV-visible spectrums were measured by Agilent 8453 UV-visible diode array spectrometer (Agilent, USA).

2. Fabrication of ILs-based EVFLL and Experiment Device.

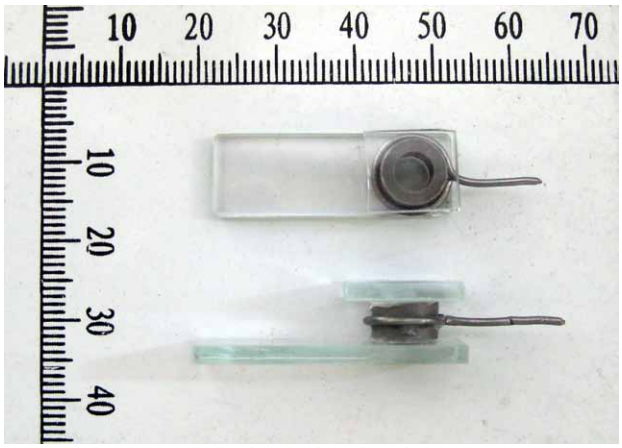

Figure S2. Picture of ILs-based EVFLL

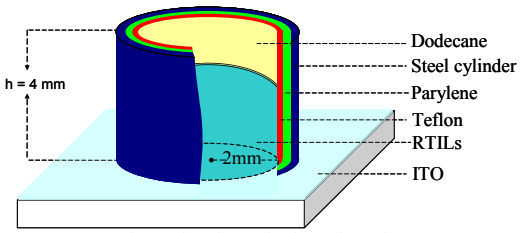

Figure S3. Schematic of a typical ILs-based EVFLL

The schematic of a typical ILs-based EVFLL is shown in Figure S3. An insulating layer of Parylene N was deposited on the steel cylinder (4 mm ×Φ 4 mm) by chemical vapor deposition (10 μm, ε_r=2.65). Subsequently a thin hydrophobic layer top coating was deposited by dip-coating as follows: the insulating layer was immersed in a 4% (w/v) of Teflon AF 1600 (DuPont) in FC 75. The substrate was withdrawn from the solution at a constant speed of 750 μm/s and the procedure was repeated twice. The resulted Teflon-covered steel cylinder were heat-treated for 6 minutes at 112 °C, and 5 minutes at 165 °C, in order to remove residual solvent and improve the adhesion of the Teflon layer to the substrate, which given a very thin Teflon coating (0.9 μm, ε_r=1.93) as a top layer to obtain the desired hydrophobic and low hysteresis properties. An ILs droplet (~20 μL) was injected in the cylinder through a 10 μL syringe. Then dodecane was transferred into the cylinder with a pipette immediately in order to reduce moisture. Both the top glass and bottom glass plates covered with ITO are glued onto the cylindrical steel with ultraviolet plastic. All ILs-based EVFLL were sealed up and tested at room temperature.

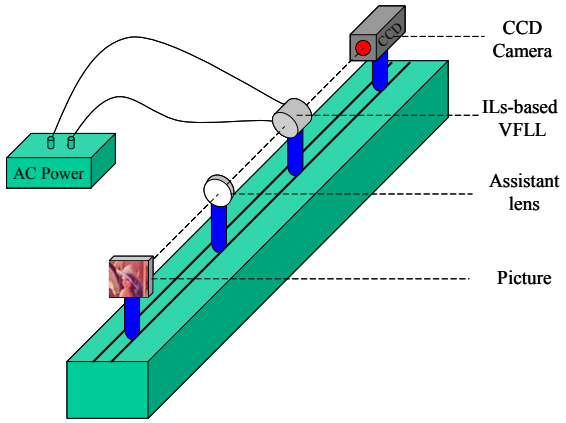

Figure S4. Experimental setup for ILs-based EVFLL imaging device used in this work

All parts are set on the guide rail. CCD camera captures the image of "Lena" through the ILs-based EVFLL and the Assistant lens which is added to assist in converging light for ILs-based EVFLL. Instead of DC, an AC power supply is chosen for several distinctive reasons as follows: First, the occurrence of the contact-angle saturation, which is still one of the most puzzling phenomena in electrowetting, is delayed in the AC case. Second, the AC case has a less contact-angle hysteresis. Third, ion-adsorption at the liquid substrate interface may be reduced with AC signal. The focal length of ILs-based EVFLL varies with the voltage of AC power supply. All voltages in this paper are root-mean-square (RMS) values.

Temperature was controlled by methylsiliconeoil bath through a thermocouple probe connected on the Digital Temperature Controller.

As shown in Figure S4, the video of light spot variation was captured by a high speed CCD camera, and then divided into frames through software. The responding time was counted by cumulating slot time.

In this work, focal length was measured by parallel light focus method (Figure S5). Make parallel light generated by laser collimator along the axis direction and transmit through the ILs-based EVFLL, then place an optical screen in another side. Adjust the screen location to ensure the spot smallest and brightest at the same time, consequently, the distance between the lens and the screen is the focal length of the lens.

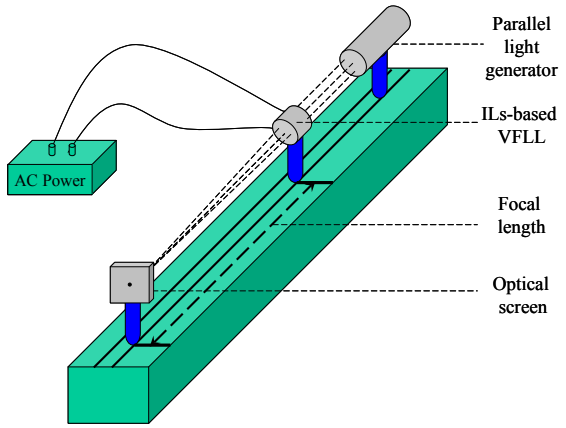

Figure S5. Experimental setup for focal length measurement in this work

3. Equations Derivation.

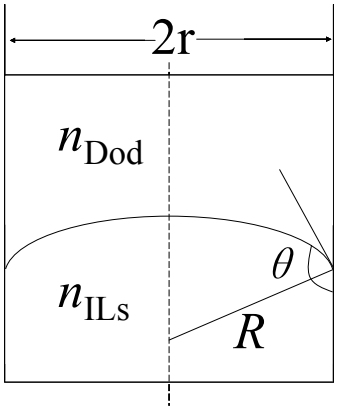

Figure S6. Model of a typical ILs-based EVFLL

Definitions of Terms

f = focal length of lens
n_{Dod} = refractive index of dodecane
n_{ILs} = refractive index of ILs
r = radius of the cylinder
R = radius of the meniscus curvature
ε_r = dielectric constant of double layers
d = double layers thickness
V = applied external voltage (RMS)
θ_0 = initial contact angle at zero voltage
$\sigma_{Tfl\text{-}ILs}$ = interfacial tension between Teflon and ILs
$\sigma_{Tfl\text{-}Dod}$ = interfacial tension between Teflon and dodecane
$\sigma_{ILs\text{-}Dod}$ = interfacial tension between ILs and dodecane
σ_{ILs} = surface tension of ILs

It could be obtained from applied optics that,

$$f = \frac{R}{n_{ILs} - n_{Dod}} \tag{S1}$$

Considering,

$$R = -\frac{r}{\cos\theta} \tag{S2}$$

And Young-Lippmann equation can be given as

$$\cos\theta = \frac{\sigma_{Tfl\text{-}ILs} - \sigma_{Tfl\text{-}Dod}}{\sigma_{ILs\text{-}Dod}} + \frac{\varepsilon_0\varepsilon_r}{2d\sigma_{ILs\text{-}Dod}}V^2 = \cos\theta_0 + \frac{\varepsilon_0\varepsilon_r}{2d\sigma_{ILs\text{-}Dod}}V^2 \tag{S3}$$

Therefore, f can be written as,

$$f = \frac{1}{\left(\frac{n_{Dod} - n_{ILs}}{r}\right)\left(\cos\theta_0 + \frac{\varepsilon_0\varepsilon_r}{2d\sigma_{ILs\text{-}Dod}}V^2\right)} \tag{S4}$$

It can be represented as,

$$f = F\left(n_{Dod}, n_{ILs}, r, \theta_0, \varepsilon_r, d, \sigma_{ILs\text{-}Dod}, V\right) \tag{S5}$$

If we set $a = (n_{Dod} - n_{ILs})\cos\theta_0 / r$, $b = (n_{Dod} - n_{ILs})\,\varepsilon_0\varepsilon_r / 2rd\sigma_{ILs\text{-}Dod}$, and $\alpha = b / a = \varepsilon_0\varepsilon_r/(2d\sigma_{ILs\text{-}Dod}\cos\theta_0)$, f could also be written as

$$f = \frac{1}{a + bV^2} = \frac{r}{\left(n_{Dod} - n_{ILs}\right)\cos\theta_0\left(1 + \alpha V^2\right)} \tag{S6}$$

According to equation S4, for a given ILs-based EVFLL, where n_{Dod}, r, ε_r and d remain constant, considering θ_0 is a function of $\sigma_{ILs\text{-}Dod}$ and $\sigma_{ILs\text{-}Dod}$ is directly proportional to σ_{ILs}, so f depends only on n_{ILs}, σ_{ILs}, and V.

$$f = \left(n_{ILs}, \sigma_{ILs}, V\right) \tag{S7}$$

Initial focal length at zero voltage f_0 can also be obtained as,

$$f_0 = \frac{1}{\left(\frac{n_{Dod} - n_{ILs}}{r}\right)\left(\frac{\sigma_{Tfl\text{-}ILs} - \sigma_{Tfl\text{-}Dod}}{\sigma_{ILs\text{-}Dod}}\right)} \tag{S8}$$

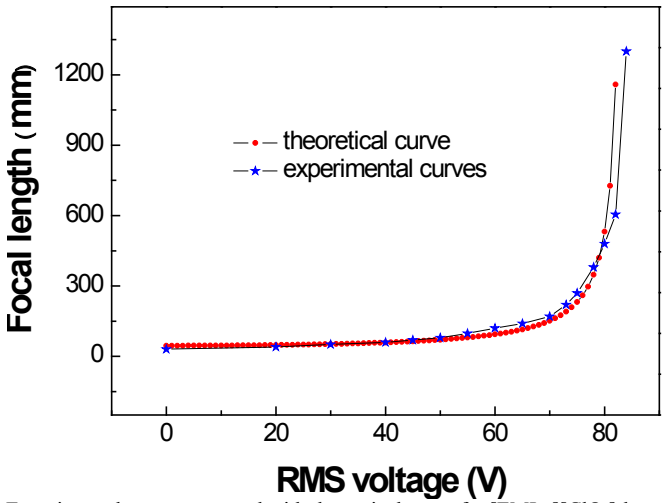

Figure S7. Experimental curve compared with theoretical curve for [EMIm][ClO_4]-based EVFLL.

Take [EMIm][ClO_4]-based EVFLL for example, the experimental result is consistent with the theoretical values closely.

4. Surface tension, viscosity, absorbance and refractive index measurements.

The data in Figure S8 and S9 and Table S1 are experimental measurement results of viscosity, surface tension and refractive index at different temperatures for seven kinds of ILs.

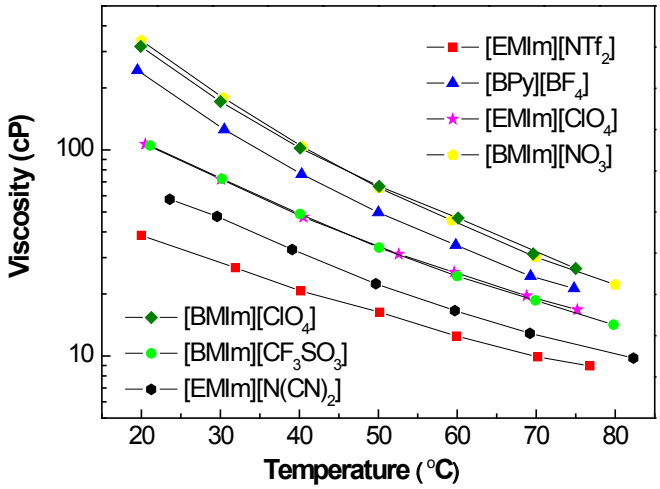

Figure S8. Viscosity versus temperature for seven different kinds of ILs.

The viscosity of ILs drops sharply with temperature ascending, which shortens responding time of ILs-based EVFLL.

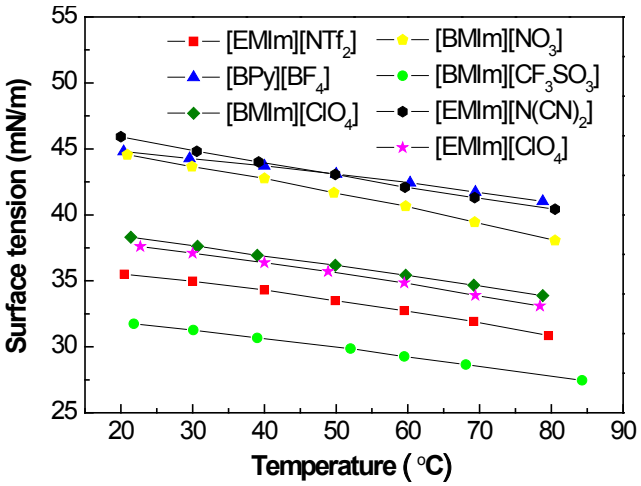

Figure S9. Surface tension versus temperature for seven different kinds of ILs.

The surface tension decreases linearly with the temperature ascending, which means that it costs less voltage to get the same focal length when the temperature rises.

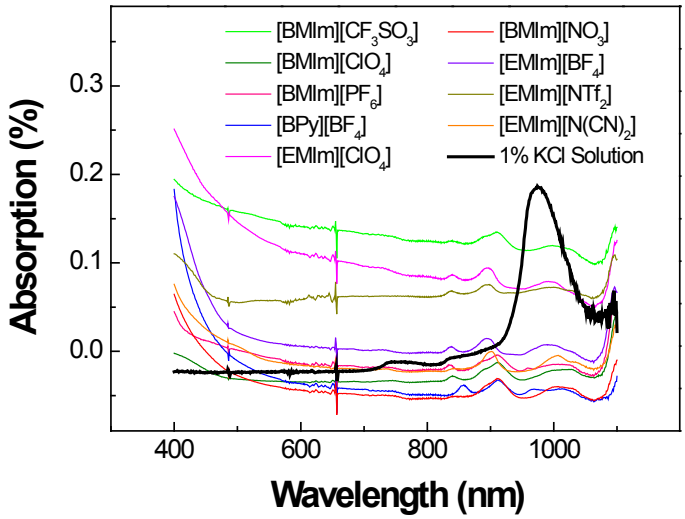

Figure S10. Absorption of ILs, dodecane and saline for wavelength between 400 and 1100 nm.

The absorption of most ILs-based EVFLL in visible light and near-infrared (400 ~ 1100 nm) is not strong. However, there is an intensive absorption around 0.9 μm by saline which would limit the imaging performance of saline-based EVFLL in near-infrared area.

Table S1. Refractive index and surface tension of ILs.

ILs	Refractive Index		Surface tension (mN/m)	
	nD^{20}	nD^{80}	σ^{20}	σ^{80}
[BMIm][PF_6]	1.4089	1.3966	39.3	35.1
[EMIm][BF_4]	1.4098	1.3978	49.0	44.2
[EMIm][NTf_2]	1.4214	1.4096	35.5	30.8
[BPy][BF_4]	1.4361	1.4223	44.8	40.9
[BMIm][CF_3SO_3]	1.4451	1.4347	31.9	27.1
[BMIm][ClO_4]	1.4709	1.4593	38.3	33.6
[EMIm][ClO_4]	1.4754	1.4636	37.8	32.9
[BMIm][NO_3]	1.4962	1.4837	44.6	38.0
[EMIm][$N(CN)_2$]	1.5329	1.5197	45.9	40.4

The refractive index and surface tension of ILs are shown in Table S1. The refractive index values are distributed from 1.4089 to 1.5329 at 20 °C and all higher than that of dodecane (1.4190) except for [EMIm][BF_4] and [BMIm][PF_6]. Besides, both the refractive index and surface tension of ILs becomes lower with temperature ascending.

5. Focal length at different voltages for ILs-based EVFLL

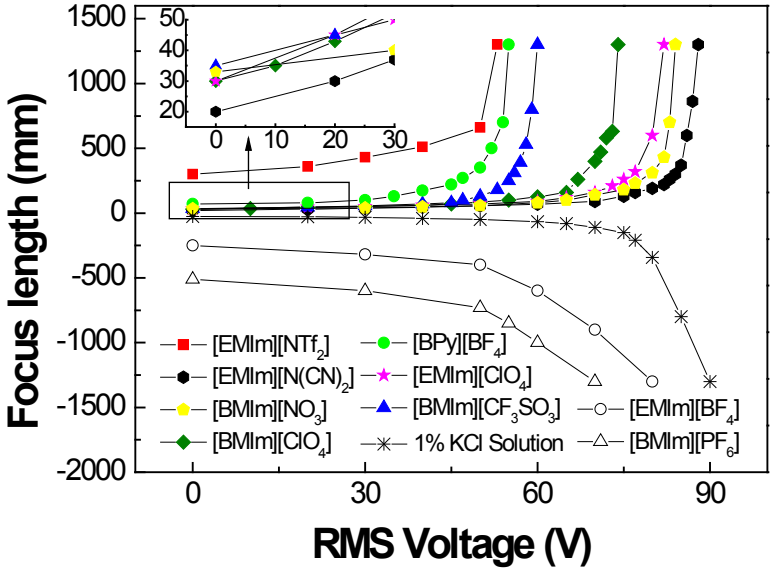

Figure S11. Change of focal length of ILs and saline-based EVFLL with applied voltage at room temperature.

It could be observed from Figure S11 that positive focal length (f>0) was obtained for most ILs-based EVFLL with short initial focal length at zero voltage and thus larger focus range. However, [EMIm][BF_4] and [BMIm][PF_6] exhibit negative focal length (f<0), similar to saline-based EVFLL. Different with the other ILs mentioned above, [EMIm][BF_4] and [BMIm][PF_6] exhibit lower refractive index than dodecane (1.4190). So the ILs-based EVFLL consisted of [EMIm][BF_4] or [BMIm][PF_6] is concave lens, which is the same with conventional liquid lens.

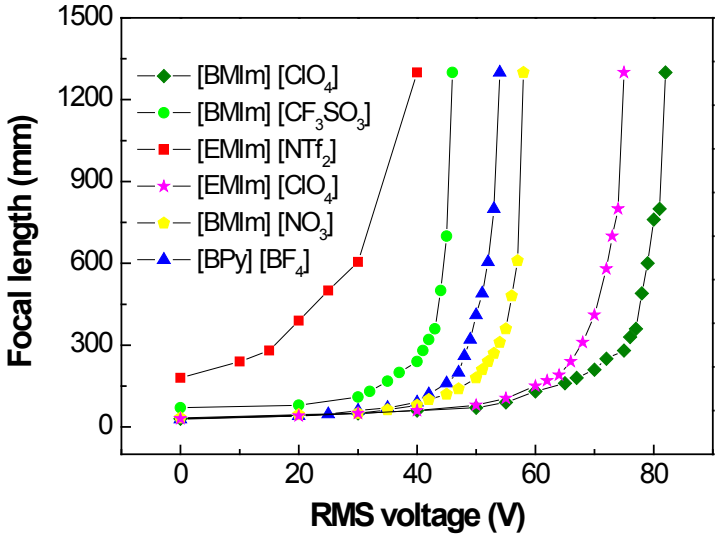

Figure S12. Focal length versus voltage for six different kinds of ILs-based EVFLL at 80°C.

[EMIm][$N(CN)_2$] with low viscosity, high refractive index and high surface tension is liable to give fast response, wide range of variable focus, etc. However the instability of [$N(CN)_2$] group at high temperature leads to color changing, which makes [$N(CN)_2$] based ILs can not be used when the temperature is higher than 60°C.

6. Power consumption

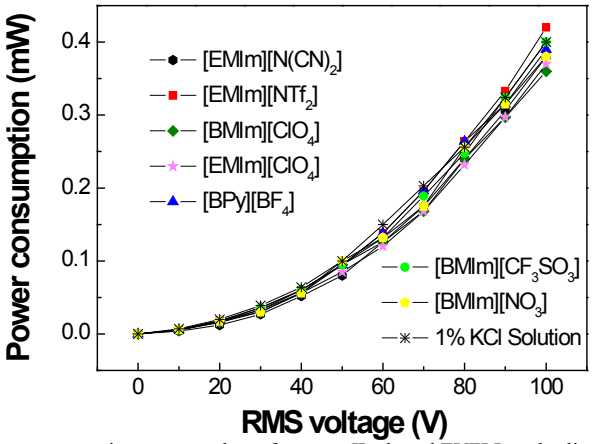

Figure S13. Power consumption versus voltage for seven ILs-based EVFLL and saline-based EVFLL

From the figure above, it could be obtained that the power consumptions of ILs-based EVFLL were all lower than that of saline-based EVFLL except for [EMIm][NTf_2]-based EVFLL.

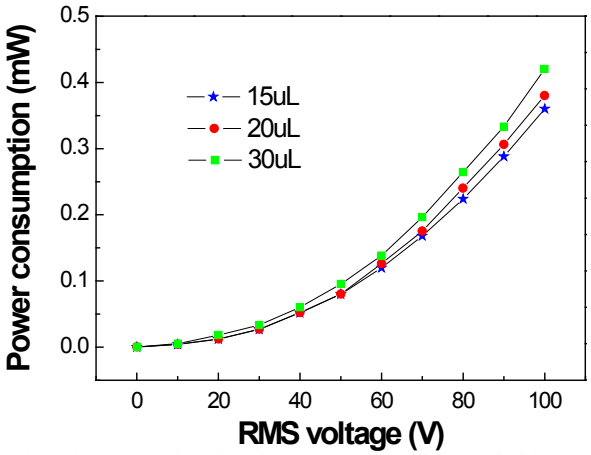

Figure S14. Power consumption of [EMIm][ClO_4]-based EVFLL versus voltage with different volume of [EMIm][ClO_4]

Changing volume of [EMIm][ClO_4] 15μL, 20μL and 30μL, respectively, it could be concluded that ILs-based EVFLL with lager volume of ILs consumes higher power. This is probably due to the more amounts of ILs, the more energy needed to drive ions arrangement.

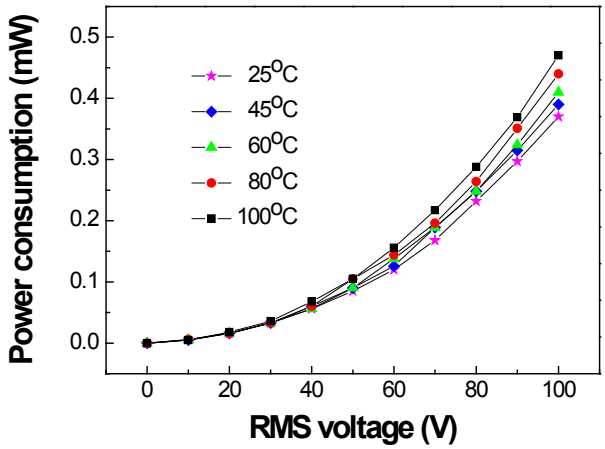

Figure S15. Power consumption of [EMIm][ClO_4]-based EVFLL versus voltage at different temperatures

In order to investigate the relationship of power consumption associated with temperature, the power consumption of ILs-based EVFLL consisted of 20μL [EMIm][ClO_4] were tested at different temperatures. From the figure above, it could be seen that high temperature leads to high power consumption. Presumably, high temperature leads to thermal motion of molecular and conductivity enhancement. Consequently, leakage current increases. And then, power consumption becomes higher.